ISSN (Print) 1226-1750
ISSN (Online) 2233-6656
Journal of Magnetics 20(3), 201-206 (2015) http://dx.doi.org/10.4283/JMAG.2015.20.3.201

Magnetic Properties of Ni/BN/Co Trilayer Structure: A First Principles Study

Arqum Hashmi and Jisang Hong*

Department of Physics, Pukyong National University, Busan 608-737, Korea

(Received 22 June 2015, Received in final form 27 July 2015, Accepted 31 July 2015)

Using the Vienna ab initio simulation package (VASP) incorporating both semiempirical and nonlocal van der Waals interaction, the structural, adsorption, and magnetic properties of Ni/BN/Co systems were investigated. We proposed that the relative spin direction of Ni and Co magnets can be easily tuned, because the total energy difference between ferromagnetic (FM) and antiferromagnetic (AFM) states is small. Despite this feature, very interestingly, both Ni and Co layers manifest half-metallic state, whereas the spacer BN layer becomes weak metal for one monolayer (ML) thickness and an insulating barrier for two ML thicknesses. The half-metallic behavior of the magnetic layers seems very robust, because it is independent of the magnetic coupling between Ni and Co. This finding indicates that the Ni/BN/Co system can be used as a potential candidate for tunneling magnetoresistance system.

Keywords : van der Waals interaction, half-metallic state, spacer layer

1. Introduction

The magnetic properties of thin films and magnetic multilayers have been extensively investigated owing to their potential applications in nanodevices and fundamental interests. For instance, low-dimensional magnetic systems is used as high-density magnetic information storage, spin filtering sensors, and magnetic random memory access [1-5]. In thin film systems, the magnetic property is well known to strongly depend on the alteration of the geometry and the underlying electronic structure.

Hexagonal boron nitride (h-BN) has a band gap energy of 5 eV and is known to bind with many transition metals. The interaction of the BN layer with metal surfaces has been well studied [6-15]. Experimentally, a single layer and multilayers of BN on different metallic substrates have been successfully synthesized. Recently, it has been proposed that a BN sheet can be used as a spacer for the magneto resistive junctions with 100% magnetoresistance (MR) ratio [16, 17]. Therefore, the study of the structural, electronic, and magnetic properties of metals with BN will be interesting. From a theoretical point of view, it is not adequate to describe the physical properties of the hybridized system of metal and layered-structure material by using the conventional exchange and correlation functions such as the local density approximation (LDA) or generalized gradient approximation (GGA) method. For example, the adsorption energy calculation by the LDA and GGA methods shows that the graphene/BN, graphene/Ni, and Ni/BN hybridized structures cannot be stable, and the same feature is found in the BN layer on Co metal surface [18], and such hybridized systems have been synthesized [19-21]. This discrepancy between the theory and experiment stems from an inaccurate description of the exchange and correlation for the layered-structure materials. Recently, the importance of van der Waals interaction in such materials has been discussed, and mostly four different types of van der Waals density functional theory, namely, DFT-D2, vdW-DF2, optPBE-vdW, and optB88-vdW [22-26], are widely used. However, extensive and systematic studies for potential spintronics by using the state-of-the-art van der Waals density functional theory are rarely reported. In this regard, our objective was to investigate the structural, adsorption, and magnetic properties of Ni/BN/Co systems by the van der Waals density functional method.

2. Numerical Method

The Vienna ab initio simulation package (VASP) [27, 28] using a plane wave basis set was used. The core

*Corresponding author: Tel: +82-51-629-5573
Fax: +82-51-629-5549, e-mail: hongj@pknu.ac.kr

electron interactions were described using the projector augmented wave (PAW) methods. The self-consistent calculations were carried out with 23 × 23 × 1 k-mesh, at a vacuum distance of 15 Å. The structure optimization was performed until the residual forces on individual atoms were < 0.01 eV $Å^{-1}$. The convergence criterion for energy was set to 0.1 meV. All the reported results were obtained at a very high plane-wave energy cut-off of 700 eV. Both semiempirical (DFT-D2) and nonlocal van der Waals (opt-PBE) interactions were used, and the structure optimization was performed via energy and force minimization procedures. Moreover, the FM and AFM spin configurations were considered to find out the magnetic ground state. To understand the role of the BN thickness, ground state adsorption geometry and the effect of the substrate on adsorption energy, the BN thickness was changed from one monolayer (ML) to two MLs; the thickness of the Ni layer was also varied from one ML to two ML coverage. Herein, the BN layers were assumed to follow the bulk h-BN structure so that AB stacking between the two BN layers could be considered in our calculation. In contrast, the Co layer was fixed to two MLs. Consequently, we explored the following systems: Ni(1ML)/BN(1ML)/Co(2ML), Ni(1ML)/BN(2ML)/Co(2ML), Ni(2ML)/BN(1ML)/Co(2ML), and Ni(2ML)/BN(2ML)/Co(2ML). The two MLs of Co are considered as the substrate layers, and the lattice constant of Co(111) (2.506 Å) was used in our calculations. Thus, the Ni and BN over layers were assumed to grow pseudomorphically on the Co substrate. The lattice constants of Co, BN and Ni are very close to each other, and thus the overall induced strain in the BN and Ni lattice was < 1%.

3. Numerical Results

The optimized structure of the BN/Co systems was already reported in the literature [18, 29], Indicating that the N atom was located on the top of Co atoms, whereas

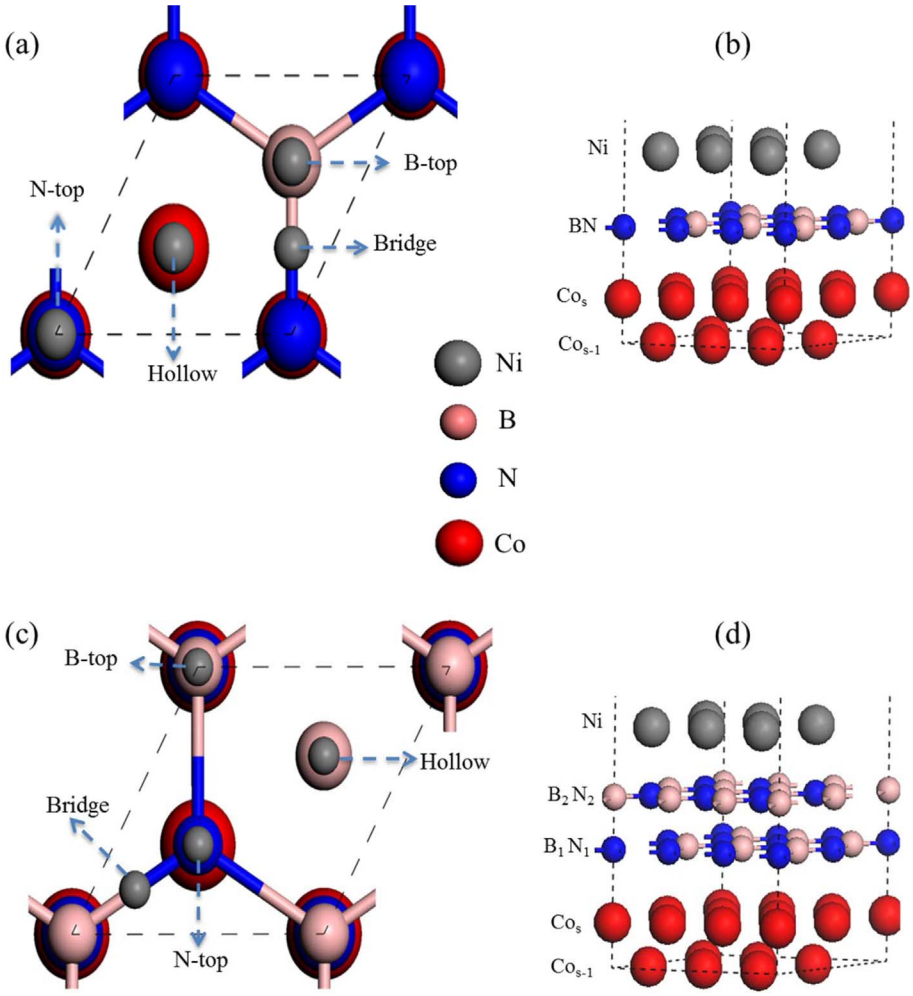

Fig. 1. (Color online) Adsorption structures of (a) top view for Ni(1ML)/BN(1ML)/Co(2ML) (b) side view of Ni(1ML)/BN(1ML)/Co(2ML) (c) top view of Ni(1ML)/BN(2ML)/Co(2ML) (d) side view of Ni(1ML)/BN(2ML)/Co(2ML).

Table 1. Calculated total energies (in meV/cell). The error bar in our calculations was in the range of ± 0.1 meV.

	DFT-D2		optPBE-vdW	
	FM	AFM	FM	AFM
Ni(1ML)/BN(1ML)/Co(2ML)				
B-top	0	1	0	1
N-top	–4	–1	1.0	3.0
Hollow	–4	–5	6.0	7.0
Bridge	0	2	2.0	3.0
Ni(1ML)/BN(2ML)/Co(2ML)				
B-top	0	0	0	–0.3
N-top	–11	11	–1	–0.9
Hollow	–10.2	10.6	3.6	2.7
Bridge	–5.1	5.2	0	0

Table 2. Calculated interlayer distance of Ni(1ML)/BN(1ML)/Co(2ML) and Ni(1ML)/BN(2ML)/Co(2ML) (in Å).

	B-top	N-top	Hollow	Bridge
Ni(1ML)/BN(1ML)/Co(2ML)				
Ni–B	2.966	2.973	2.961	2.998
Ni–N	2.899	2.907	2.906	2.939
N–Co_S	2.353	2.122	2.121	2.121
B–Co_S	2.110	2.056	2.066	2.062
Co_S–Co_{S-1}	1.882	1.877	1.876	1.878
Ni(1ML)/BN(2ML)/Co(2ML)				
Ni–N_2	3.042	3.014	3.000	3.044
Ni–B_2	3.019	2.991	2.975	3.021
N_2–N_1	2.933	2.933	2.929	2.933
B_2–N_1	2.957	2.956	2.953	2.957
N_1–Co_S	2.105	2.105	2.104	2.105
B_1-Co_S	2.003	1.998	1.999	2.001
Co_S –Co_{S-1}	1.874	1.876	1.875	1.876

the B atoms resided in the fcc sites [18, 29]. Herein, by taking the advantage of these results, the adsorption site of the Ni layer on BN/Co(111) was easily found. Fig. 1 shows the schematic illustrations of four possible adsorption sites of the Ni layer such as N-top, B-top, hollow, and bridge sites for Ni(1ML)/BN(1ML)/Co(2ML) and Ni(1ML)/BN(2ML)/Co(2ML). The red, blue, pink, and gray balls stand for Co, N, B, and Ni atoms, respectively. For Ni(2ML)/BN(2ML)/Co(2ML), we assumed that the stacking of the second Ni layer followed the pristine Ni (111) structure. The two Co (Ni) layers preferred to ferromagnetically couple to each other. Hence, the FM and AFM configurations between the Co and Ni layers separated by a BN spacer were investigated.

The total energy of B-top with the FM state was set to zero as the reference. As listed in Table 1, the total energy calculations were not consistent, because the ground state adsorption site varies according to the van der Waals interaction types used for the total energy calculations. Moreover, the energy difference between the two magnetic states (FM and AFM states) was rather small. This finding indicates that the most stable adsorption structure and the relative magnetization of the two magnets may depend on the sample growth conditions. Moreover, our results show that the exact description of van der Waals interaction still remained an open question and need further investigation. However, despite this inconsistency in the ground state structure, the Ni/BN/Co system was stabilized via the adsorption energy calculation. The adsorption energy (E_{ads}) was obtained by using the following equation.

$$E_{ads} = E_{BN/Co} + E_{Ni} - E_{Ni/BN/Co} \quad (1)$$

where $E_{BN/Co}$ and E_{Ni} are the total energy of the BN/Co hybridized system and the total energies of the free-standing Ni layer, respectively, and $E_{Ni/BN/Co}$ is the total energy of the Ni/BN/Co hybridized system. The calculated adsorption energies of Ni(1ML)/BN(1ML)/Co(2ML) were ~280 and 213 meV by the DFT-D2 and optPBE-vdw methods, respectively, and this result was substantially different, because the hybridized systems were not stable when the LDA and GGA methods were used. For Ni(1ML)/BN(2ML)/Co(2ML), the calculated adsorption energies were 218 and 157 meV by the DFT-D2 and optPBE-vdw methods, respectively. Overall, the Ni layer was physisorbed on the BN/Co system, and the optimized interlayer distances were found by the DFT-D2 method in Table 2. The general trend of the interlayer distances calculated by other van der Waals interactions was almost the same. For Ni(1ML)/BN(1ML)/Co(2ML) system, the buckling behavior was found in the BN layer. More specifically, the B atoms moved to the Co side, whereas the N atoms were repelled from the Co layer. This buckling feature of BN agreed well with the previous study [29]. In Ni(1ML)/BN(2ML)/Co(2ML) structure, the buckling feature was found in the BN layer adjacent to Co_S, whereas the second BN layer next to Ni was almost flat. Thus, the buckling effect occurred only in the nearest neighbor layer from the Co substrate. As described earlier, the adsorption energy was suppressed in Ni(1ML)/BN(2ML)/Co(2ML) as compared to that in Ni(1ML)/BN(2ML)/Co(2ML), because of the buckling of the BN layer. The same phenomenon for the adsorption energy because of the geometrical effect of the BN layer was observed in the graphene/BN/Co (111) systems [18].

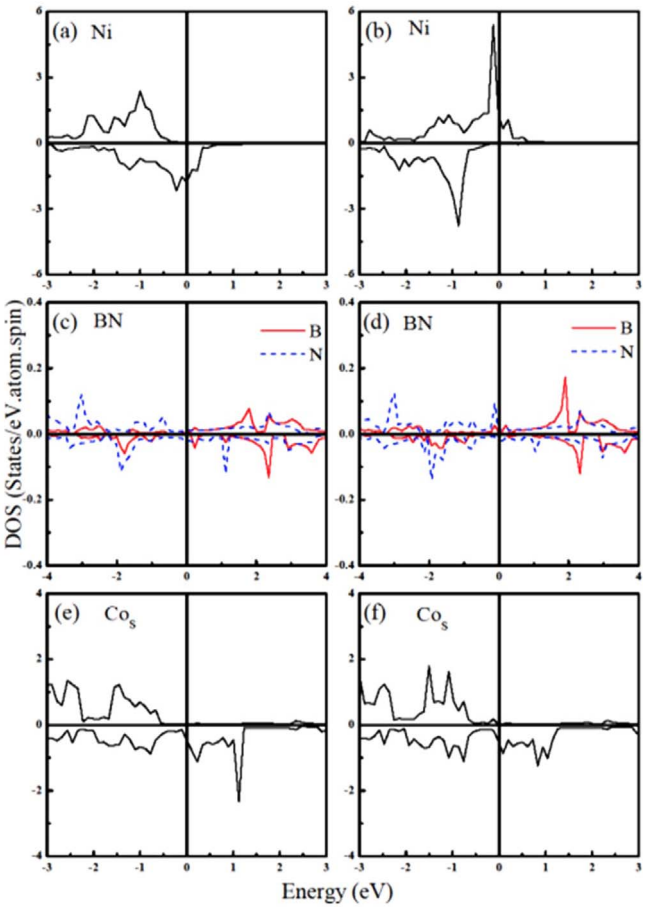

Fig. 2. (Color online) Calculated DOS of Ni, BN, and Co in Ni(1ML)/BN(1ML)/Co(2ML): (a), (c), and (e) DOS of Ni, BN, and Co_s in the FM state, respectively, whereas (b), (d), and (f) DOS of Ni, BN, and Co_s, respectively, for the AFM configuration.

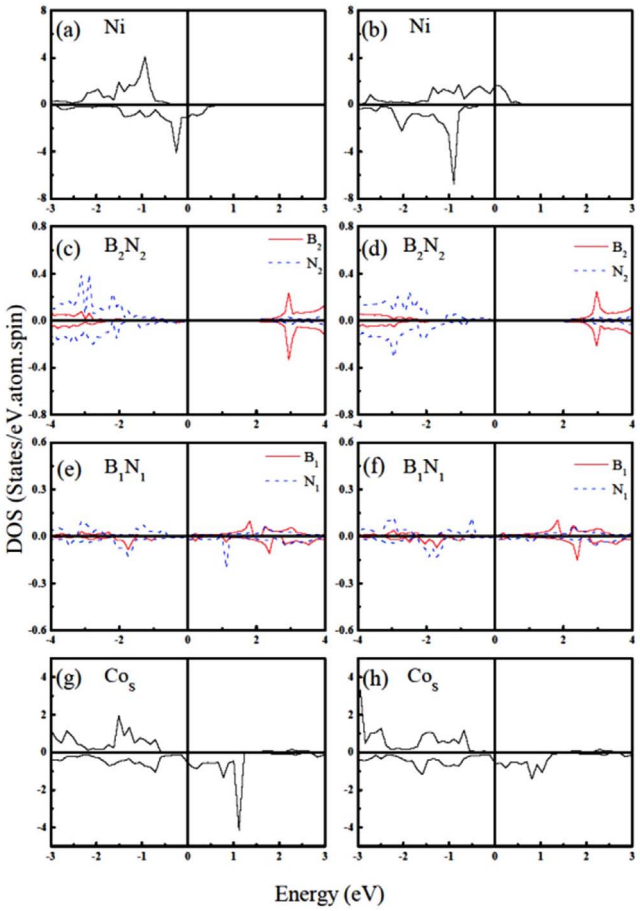

Fig. 3. (Color online) Calculated DOS of Ni, BN, and Co in Ni(1ML)/BN(2ML)/Co(2ML): DOS in the FM configuration of (a) Ni (c) 2nd BN layer (e) 1st BN layer and (g) Co_s interface layer, whereas (b) Ni (d) 2nd BN layer (f) 1st BN layer, and (h) Co_s interface layer DOS in the AFM configuration.

The calculated density of the states (DOS) of each system was obtained by the DFT-D2 method. Fig. 2 shows the DOS of the FM and AFM spin configurations of Ni(1ML)/BN(1ML)/Co(2ML). First, half-metallic states were clearly observed for both the Co and Ni layers, and the single BN layer shows metallic state, but the DOS at the Fermi level is quite weak. In the AFM configuration, both the magnetic layers and BN still showed the same trend except the change in the relative spin direction between the Ni and Co magnets. Fig. 3 shows the DOS of Ni(1ML)/BN(2ML)/Co(2ML). The essential feature was still maintained in both the Ni and Co layers, and this was again independent of the relative spin direction of the magnetic layers. However, in this case, the BN adjacent to Ni became an insulating layer, whereas the BN layer next to the Co layer showed a weak metallic state; however, the DOS at the Fermi level was almost negligible. For all the systems with different functionals, both Co_{s-1} and Co_s had the magnetic moments in the range 1.71-1.75 and 1.61-1.69 μ_B inside the Wigner-Seitz radius, respectively. In contrast, Ni showed a magnetic moment in the range 0.79-0.83 μ_B inside the Wigner-Seitz radius. Because of the magnetic Co layer at the interface between Co and BN, small magnetic moments in the range –0.014 and 0.013 μ_B were observed for B and N atoms, and this was independent of the relative spin direction in the Ni layer. As indicated above, the magnetic moment of Co is much larger than that of Ni, indicating that the induced magnetic moment in the BN layer is mostly affected by the Co layer, and this behavior is clearly seen from the DOS. Our calculated DOS and magnetic moments are well in accordance with each other.

Fig. 4 shows the DOS of Ni(2ML)/BN(2ML)/Co(2ML) system, showing the similar behavior. As a result, a half-metallic state, independent of film thickness, was observed. The same behavior was observed with the different van

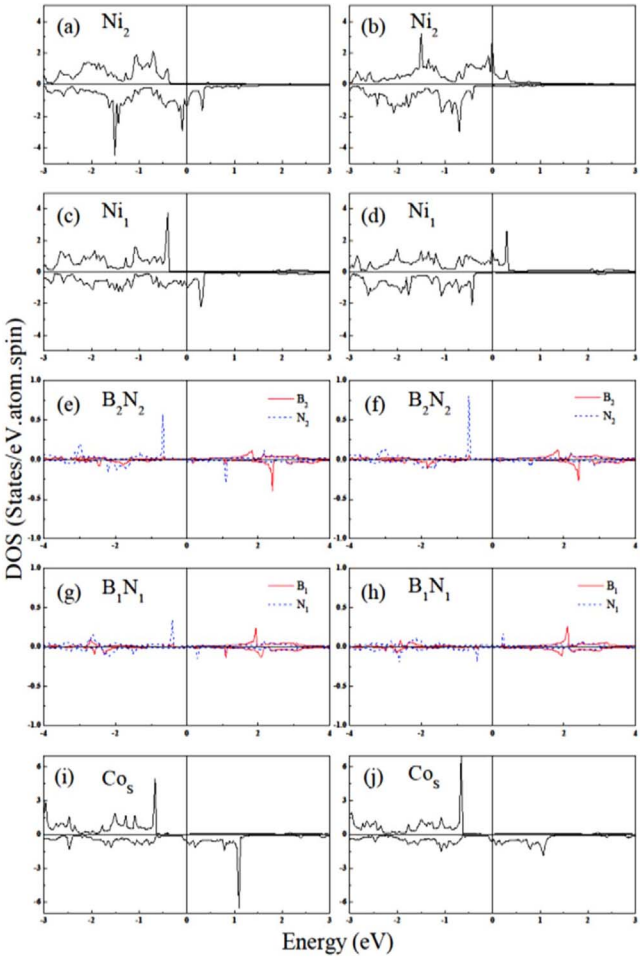

Fig. 4. (Color online) Calculated DOS of Ni, BN, and Co in Ni(2ML)/BN(2ML)/Co(2ML): DOS in the FM configuration of (a) 2nd Ni layer (c) 1st Ni layer (e) 2nd BN layer (g) 1st BN layer, and (i) Co_s interface layer, whereas (b) 2nd Ni layer (d) 1st Ni layer (f) 2nd BN layer (h) 1st BN layer, and (j) Co_s interface layer DOS in the AFM configuration.

der Waals approaches, but the calculated results are not shown here. For spin dependent transport in a magnetic tunnel junction structure, the electronic structure at the interface plays an essential role. Thus, the half metallicity observed in this system can provoke very interesting issues for tunneling magnetoresistance (TMR) or spin injection studies. Because of the half-metallic behavior at the interface layer and the insulating character of the BN layer, a high TMR ratio was expected for this structure. The AFM state can be achieved in some cases because of the rather small energy difference. Nonetheless, this will not cause any problem for a high TMR ratio. In an asymmetric structure such as in our system, the coercivity field of one magnetic layer will be smaller than that of the other layer, and the relative magnetization will be easily tuned, resulting in the same physics.

4. Summary

In conclusion, the structural, adsorption, and magnetic properties of Ni/BN/Co systems were investigated using both the semiempirical and nonlocal van der Waals interactions. The adsorption of the Ni/BN/Co system showed a stable structure, whereas the conventional calculations by the LDA or GGA methods fail to explain such adsorption. The buckling of the BN spacer layer was affected by the Co layer, thus enhancing the adsorption energy; however, the effect of buckling is limited only to the nearest neighbor with respect to the Co substrate. Interestingly, both the Ni and Co magnetic layers show half-metallic states, and in particular this half metallicity at the interface is independent of the relative magnetization of Ni and Co and film thickness. This finding may indicate that the Ni/BN/Co structures can be an ideal system for a large magnetoresistance, because one spin current will be significantly suppressed, resulting in a large TMR ratio.

Acknowledgments

This study was supported by the Basic Science Research Program through the National Research Foundation of Korea (NRF) funded by the Ministry of Education, Science and Technology (No. 2013R1A1A2006071) and by the Supercomputing Center/Korea Institute of Science and Technology Information with supercomputing resources including technical support (KSC-2015-C3-021).

References

[1] J.-G. (Jimmy) Zhu and C. Park, Materials Today **9**, 36 (2006).
[2] C. Heiliger, P. Zahn, and I. Mertig, Materials Today **9**, 46 (2006).
[3] O. V. Yazyev and M. I. Katsnelson, Phys. Rev. Lett. **100**, 047209 (2008).
[4] F. Muoz-Rojas, J. Fernndez-Rossier, and J. J. Palacios, Phys. Rev. Lett. **102**, 136810 (2009).
[5] O. V. Yazyev, Nano Lett. **8**, 1011 (2008).
[6] A. B. Preobrajenski, A. S. Vinogradov, and N. Mrtensson, Surface Science **582**, 21 (2005).
[7] M. Morscher, M. Corso, T. Greber, and J. Osterwalder, Surface Science **600**, 3280 (2006).
[8] A. B. Preobrajenski, A. S. Vinogradov, M. L. Ng, E. avar, R. Westerstrm, A. Mikkelsen, E. Lundgren, and N. Mrtensson, Phys. Rev. B **75**, 245412 (2007).
[9] M. Corso, W. Auwrter, M. Muntwiler, A. Tamai, T. Greber, and J. Osterwalder, Science **303**, 217 (2004).

[10] M. Corso, T. Greber, and J. Osterwalder, Surface Science **577**, L78 (2005).
[11] C. Oshima and A. Nagashima, J. Phys.: Condens. Matter **9**, 1 (1997).
[12] R. Laskowski, P. Blaha, and K. Schwarz, Phys. Rev. B **78**, 045409 (2008).
[13] J. G. Daz, Y. Ding, R. Koitz, A. P. Seitsonen, M. Iannuzzi, and J. Hutter, Theor. Chem. Acc. **132**, 1 (2013).
[14] M. Chen, Y.-J. Zhao, J.-H. Liao, and X.-B. Yang, Phys. Rev. B **86**, 045459 (2012).
[15] A. B. Preobrajenski, M. A. Nesterov, M. L. Ng, A. S. Vinogradov, and N. Mårtensson, Chem. Phys. Lett. **446**, 119 (2007).
[16] O. V. Yazyev and A. Pasquarello, Phys. Rev. B **80**, 035408 (2009).
[17] M. L. Hu, Z. Yu, K. W. Zhang, L. Z. Sun, and J. X. Zhong, J. Phys. Chem. C **115**, 8260 (2011).
[18] A. Hashmi and J. Hong, J. Magn. Magn. Mater. **355**, 7 (2014).
[19] K. Suenaga, C. Colliex, N. Demoncy, A. Loiseau, H. Pascard, and F. Willaime, Science **278**, 653 (1997).
[20] W. Han, W. Mickelson, and A. Zettl, Appl. Phys. Lett. **81**, 1110 (2002).
[21] T. Kawasaki, T. Ichimura, H. Kishimoto, A. A. Akbar, T. Ogawa, and C. Oshima, Surf. Rev. Lett. **9**, 1459 (2002).
[22] S. Grimme, J. Comput. Chem. **27**, 1787 (2006).
[23] K. Lee, E. D. Murray, L. Kong, B. I. Lundqvist, and D. C. Langreth, Phys. Rev. B **82**, 081101 (2010).
[24] M. Dion, H. Rydberg, E. Schröder, D. C. Langreth, and B. I. Lundqvist, Phys. Rev. Lett. **92**, 246401 (2004).
[25] A. D. Becke, Phys. Rev. A **38**, 3098 (1988).
[26] J. Klimes, D. R. Bowler, and A. Michaelides, J. Phys. Condens. Mater. **22**, 022201 (2010).
[27] G. Kresse and J. Furthmuller, Comput. Mater. Sci. **6**, 15 (1996).
[28] G. Kresse and J. Furthmuller, Phys. Rev. B **54**, 11169 (1996).
[29] Y. G. Zhouab, X. T. Zua, and F. Gaob, Solid. State. Comm. **151**, 883 (2011).